

# Real-time measurements of solar $pp$ neutrinos using $^{131}\text{Xe}$

**J Kostensalo and J. Suhonen**

University of Jyväskylä, Department of Physics, 40014 Jyväskylä, Finland

E-mail: joel.j.kostensalo@student.jyu.fi

**K Zuber**

Institut für Kern- und Teilchenphysik, TU Dresden, Zellescher Weg 19, 01062  
Dresden, Germany

E-mail: kai.zuber@tu-dresden.de

**Abstract.** Various large-scale experiments for double beta decay or dark matter are based on xenon. Current experiments are on the tonne scale but there are also ideas to aim for even larger sizes in the future. Here we study the potential of the isotope  $^{131}\text{Xe}$  to allow to make real-time measurements of solar  $pp$  neutrinos, besides classical neutrino-electron scattering. Improved nuclear models are used to determine the cross-section of neutrinos on  $^{131}\text{Xe}$ . The present calculations deviate significantly from the previous ones due to updated estimates for the excited-state contributions. The updated capture-rate estimate for  $pp$  neutrinos is  $(4.47 \pm 0.09)$  SNU and for all solar neutrinos  $(80 \pm 21)$  SNU, with neutrino survival probabilities taken into account. Depending on the amount of Xe, solar  $pp$  neutrinos might be measured with rates of 100 per day, thus allowing to monitor them in real time for a long period.

## 1. Introduction

Neutrinos play a crucial role in modern particle, nuclear and astrophysics, including cosmology [1, 2]. It has been a major achievement of the last 25 years to show that neutrinos have a non-vanishing rest mass and that the problem of missing solar neutrinos could be solved [3]. Solar-neutrino measurements are one of the most important ingredients for the understanding of the Sun, especially for the nuclear fusion processes. The low-energy region (below 1 MeV) of solar neutrinos has been observed in various radiochemical experiments starting from the famous Homestake experiment [4], as well as further radiochemical experiments based on  $^{71}\text{Ga}$ , namely GALLEX [5], GNO [6, 7] and SAGE [8], which were able to enter the energy region of the most abundant  $pp$  neutrinos. All of them were radiochemical counting experiments without any energy or time information. Hence, it is desirable to perform real-time experiments in the low-energy region. Such measurements have successfully been performed by Borexino over the last decade. Here the signal is the neutrino-electron scattering in a liquid scintillator. Due to the extremely low impurity level, Borexino was able to detect all  $pp$ -chain reactions [9], and very recently it also announced the first detection of CNO neutrinos [10]. Given the success of all these experiments, special dedicated solar-neutrino experiments will likely not be performed anymore. However, potential improvements on solar-neutrino data can still be made in a parasitic way. They are linked to astro-particle and nuclear physics which - among others - include topics like searches for dark matter or neutrino-less double beta decay. As neither of these two have been observed, experiments have to push towards larger and larger masses for a potential discovery. Thus, multi-ton-scale next-generation experiments, looking for double beta decay and dark matter, will appear. These experiments will be large enough to allow interference of solar neutrinos with the measurement signals. On the positive side, this might allow to gain more information on solar neutrinos .

Here we want to explore the potential of the new large-scale Xenon-detector experiments [11]. These kind of experiments will also detect solar neutrinos via neutrino-electron scattering - like scintillators - producing recoil electrons. Here the focus for solar neutrinos is on one particular Xenon isotope,  $^{131}\text{Xe}$ , which has a threshold of  $355 \pm 5$  keV [12] for neutrino capture. It is covering the highest 65 keV of the  $pp$  neutrinos up to the endpoint of 420 keV. The natural abundance of  $^{131}\text{Xe}$  is 21.2%. Hence, an additional neutrino reaction, besides the electron scattering, is possible via



Unfortunately, no nice coincidence can be formed as the half-life of the nuclide  $^{131}\text{Cs}$  is 9.69 days. The detection signal of  $^{131}\text{Cs}$  would be X-rays of about 30 keV and Auger electrons around 3.4 and 24.6 keV. Such a long time spread prohibits a nice coincidence. The only way of detection would be through the accumulation of  $^{131}\text{Cs}$ , combined with a sophisticated analysis of the low-energy spectrum. This might allow to identify a kind of peak by integrating the number of daughter decays.

## 2. Neutrino cross section

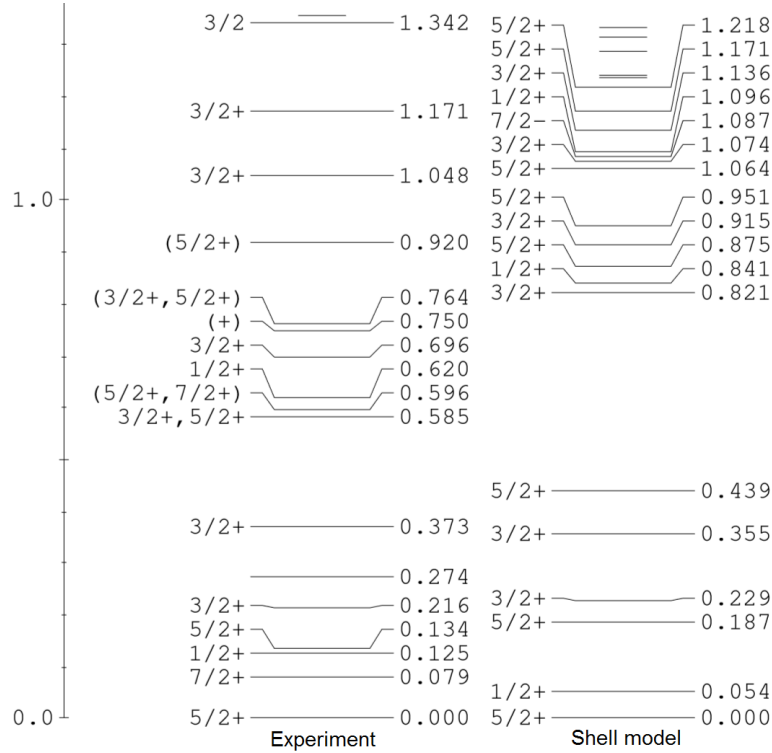


**Figure 1.** Experimental and shell-model calculated energy spectra for  $^{131}\text{Cs}$  with only the states relevant for the neutrino-nucleus scattering off the  $3/2^+$  ground state of  $^{131}\text{Xe}$  included.

The neutrino-nucleus cross-section calculations presented here are based on the Donnelly-Walecka method [13, 14] for the treatment of semi-leptonic processes in nuclei. The necessary formulae and details of the application of the formalism can also be found in [15].

Given that the threshold for the charged-current neutrino-nucleus scattering off  $^{131}\text{Xe}$  is  $355 \pm 5$  keV, we need to calculate the final states up to about 1.4 MeV in order to cover the  $pp$ ,  $pep$ ,  ${}^7\text{B}$ , and CNO neutrinos. The initial and final states for these transitions, as well as the one-body transition densities, were calculated in the shell-model framework using the computer code NuShellX@MSU [16]. The calculations were done in a model space consisting of the orbitals  $0g_{7/2}$ ,  $1d$ ,  $2s$  and  $0h_{11/2}$ , for both protons and neutrons, with the effective Hamiltonian  $\text{sn100pn}$  [17]. Due to the huge computational burden of the shell-model calculations, some truncations had to be made. For the states  $1/2_1^+$ ,  $3/2_{1,2}^+$ , and  $5/2_{\text{g.s.,}2}^+$  the neutron orbital  $0f_{7/2}$  was filled with 8 neutrons, while no restrictions were posed on the other orbitals. However, the computational burden of this truncation was too large to allow calculations of more states. Instead, a second calculation was done keeping additionally the proton orbital  $0h_{11/2}$  empty. This was done for 50 states of the spin parities  $1/2^\pm$ ,  $3/2^\pm$ ,  $5/2^\pm$ ,  $7/2^-$  in

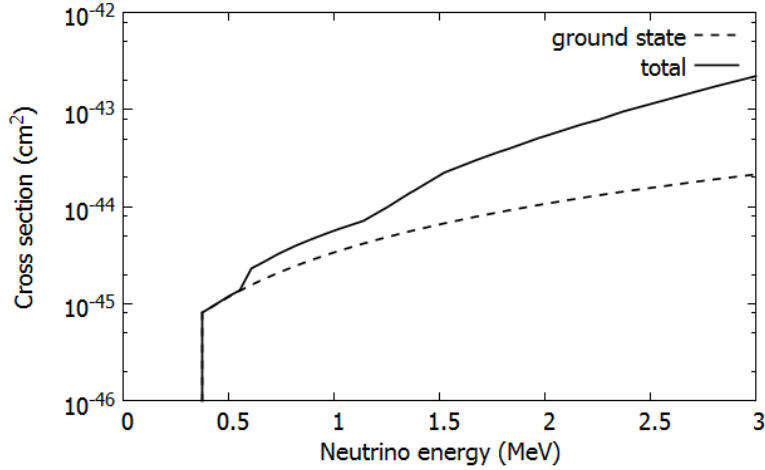


**Figure 2.** Theoretical neutrino-nucleus cross section based on our shell-model calculation. The ground-state contribution can be related to the  $^{131}\text{Cs}$  half-life and is thus known to few tenths of per cent. The  $pp$ ,  $pep$ ,  ${}^7\text{B}$ , and CNO contributions are calculated using this cross section. The maximum energy of these neutrinos is about 1.7 MeV.

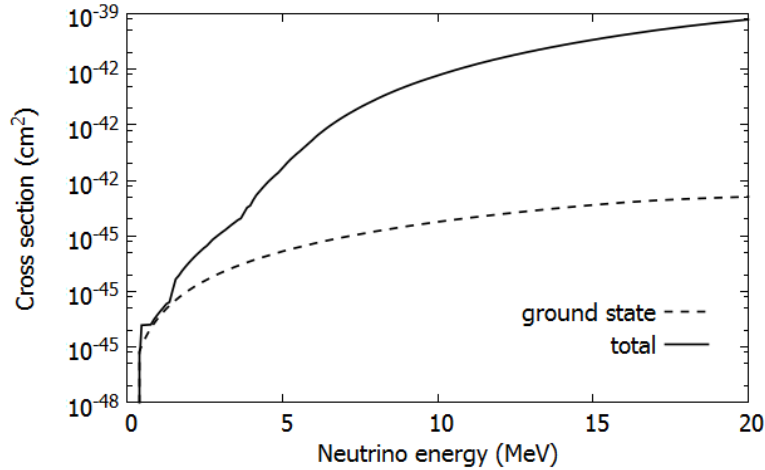


**Figure 3.** Theoretical neutrino-nucleus cross section based on the microscopic quasiparticle-phonon model (MQPM). The  ${}^8\text{B}$  and  $hep$  contributions are calculated using this cross section.

$^{131}\text{Cs}$ . The ground state of  $^{131}\text{Xe}$  was calculated in both cases with the same truncation as used for  $^{131}\text{Cs}$  in order to keep the calculations consistent. For the low energies considered here, the higher-multipole contributions are more than an order of magnitude smaller, and thus the higher-spin states are not relevant.

For  ${}^8\text{B}$  and  $hep$  neutrinos we adopt the recent cross-section results of Pirinen et al. [18], which are calculated using the microscopic quasiparticle-phonon model (MQPM) [19, 20]. MQPM is an extension of the quasiparticle random-phase approximation to odd-mass nuclei. The MQPM approach can utilize a much larger model space than

**Table 1.** The nuclear-structure model, survival probability and neutrino flux, adopted for each component of the solar-neutrino spectrum. The fluxes are from the solar model BS05(OP) [23] and survival probabilities from [24]. The last two lines give the solar-neutrino capture rates of the present work and Georgadze *et al.* [25] in units of SNU.

	$pp$	$pep$	$hep$	$^7\text{Be}$	$^8\text{B}$	$^{13}\text{N}$	$^{15}\text{O}$	$^{17}\text{F}$
Theory	SM	SM	MQPM	SM	MQPM	SM	SM	SM
Surv.	0.54	0.5	0.36	0.54	0.36	0.54	0.5	0.5
Flux	$5.99 \times 10^{10}$	$1.42 \times 10^8$	7930	$4.84 \times 10^9$	$5.69 \times 10^6$	$3.07 \times 10^8$	$2.33 \times 10^8$	$5.84 \times 10^6$
SNU (new)	4.47(9)	1.2(3)	0.33(10)	10.4(14)	62(19)	0.52(7)	0.9(2)	0.024(5)
SNU [25]	5.2	0.80	-	9.6	4.6	0.86	0.90	-

the shell model and thus for higher-energy neutrinos it is a good choice, while for the individual low-energy states the shell model is preferable.

The shell-model calculated energy spectrum of  $^{131}\text{Cs}$  is presented in figure 1. The shell model manages to predict the ground-state spin-parity correctly, as well as getting the density of states roughly right. Since the exact energies are important for the lowest energy states, we adopt the experimental energies for the excited states  $1/2_1^+$ ,  $3/2_{1,2}^+$  and  $5/2_2^+$ . Furthermore, the ground-state-to-ground-state scattering cross section can be deduced from the electron-capture half-life of  $^{131}\text{Cs}$  through the reduced transition probability  $B(\text{GT})$ , obtained from

$$B(\text{GT}) = \frac{2J+1}{2J'+1} \frac{2\pi^3 \hbar^7 \ln 2}{m_e^5 c^4 (G_F \cos \theta_C)^2} \times 10^{-\log ft} = 0.0178, \quad (2)$$

where  $J = 5/2$  is the spin of the  $^{131}\text{Cs}$  ground state,  $J' = 3/2$  is the spin of the  $^{131}\text{Xe}$  ground state,  $\theta_C \approx 13.04^\circ$  is the Cabibbo angle,  $G_F$  is the Fermi coupling constant and  $t$  is the electron-capture half-life. The value of the phase-space factor  $f = 5.548$  can be interpolated from the tables of Ref. [21]. For the rest of the states we adopt an effective value  $g_A = 1.0$  of the axial-vector coupling in order to account for the limited model space (see e.g. the review [22]).

In the paper of Pirinen *et al.* [18] the MQPM results for  $^8\text{B}$  neutrinos are given for  $g_A$  values of 0.7 and 1.0. We choose the value  $g_A = 1.0$  here but fix the ground-state-to-ground-state cross section using the half-life of  $^{131}\text{Cs}$ , as was done in the case of the shell-model calculations.

The cross section as a function of the neutrino energy has been presented for the shell model in Fig. 2 and for the MQPM in Fig. 3. For the energies relevant for  $pp$ ,  $pep$ ,  $^7\text{B}$  and CNO neutrinos, the cross section is dominated by the ground-state-to-ground-state contribution, while for  $^8\text{B}$  and  $hep$  neutrinos the excited states dominate.

The contributions for each component of the neutrino spectrum are given in Table 1. The largest contribution comes from  $^8\text{B}$  neutrinos. However, the  $pp$  and  $^7\text{B}$  contributions are individually almost as large. The  $^8\text{B}$  contribution accounts for only about 36% of the total expected events. Thus, calculating the solar-neutrino spectrum only for  $^8\text{B}$  neutrinos, as done in Ref. [18], results in a severe under prediction of the total number of events.

While the ground-state-to-ground-state contribution (which is 15.6 % of the total cross section) is known very precisely, with an uncertainty estimated here as 2 % due to the precision of the natural constants and the phase-space factor  $f$ , there are quite large uncertainties related to the other states. Assuming a conservative 30 % uncertainty, independent of the ground-state error, for the rest of the states, the total solar-neutrino capture rate for  $^{131}\text{Xe}$  is

$$R(^{131}\text{Xe}) = (80 \pm 21) \text{ SNU}, \quad (\text{Solar neutrinos}) \quad (3)$$

which has been corrected for the survival probabilities from [24], and which is much larger than the old estimate 20.0 SNU [25]. The  $pp$  neutrino capture rate is predicted to be about 14 % lower than the previous estimate. About 4 % of this difference is explained by the updated interpolation of the *logft*-value, 0.5 % by the updated flux in the new solar model, and the rest is due to the contribution of the excited states. For  $^7\text{Be}$  neutrinos the estimate for the rate is increased with respect to the previous results, owing to the increased  $^7\text{Be}$  neutrino-flux estimate in the more recent solar model [23]. However, the results are in agreement within the uncertainties. The major difference in the rates relates to  $^8\text{B}$  neutrinos, which in our updated calculations are predicted to contribute over 10 times as many counts as in the old work. This difference highlights the vast uncertainties related to the excited-state contributions.

### 3. Outlook and conclusion

We have explored the potential for solar-neutrino measurements in the  $pp$  region by using the isotope  $^{131}\text{Xe}$ . Large-scale Xe detectors are used since many years for searches of dark matter and neutrinoless double beta decay. As nothing was found so far, experiments are upgraded and are now on the ton scale, like Xenon1T [26] and LUX-ZEPLIN (LZ) [27]. Even larger detectors are planned, like the DARWIN experiment using 50 tons of Xenon [28]. Hence, such a  $pp$  measurement based on  $^{131}\text{Xe}$  might become reality.

### Acknowledgements

This work has partially been supported by Academy of Finland under the Academy project no. 318043. J. K. acknowledges the financial support from the Jenny and Antti Wihuri Foundation.

### References

- [1] H. Ejiri, J. Suhonen, K. Zuber, *Phys. Rep.* **797**,1(2019).
- [2] K. Zuber, *Neutrino Physics* 3rd edition, CRC Press 2020.
- [3] S. N. Ahmed, *Phys. Rev. Lett.* **92**,181301(2004).
- [4] B. T. Cleveland et al., *Astroph. J.* **496**,505(1998).
- [5] W. Hampel et al., *Phys. Lett.* **B 447**,127(1999).
- [6] M. Altmann et al., *Phys. Lett.* **B 616**,214(2005).
- [7] F. Kaether et al., *Phys. Lett.* **B 685**,47(2010).

- [8] J. N. Abdurashitov et al., *Phys. Rev. C* **80**,015807(2009).
- [9] G. Bellini et al., *Nature* **562**,505(2018).
- [10] G. Bellini et al., acc. by Nature
- [11] N.Barros, J. Thurn, K. Zuber *Journal of Physics G* **41**,115105(2014).
- [12] G. Audi et al., *Chin. Phys. C.*, 41, 030001, (2014).
- [13] J. S. O'Connell, T. W. Donnelly, and J. D. Walecka, *Phys. Rev. C* **6**,719(1972).
- [14] T. W. Donnelly and R. D. Peccei, *Phys. Rep.* **50**,1(1979).
- [15] E. Ydrefors and J. Suhonen, *Adv. High Energy Phys.* **2012**, 373946 (2012).
- [16] B. A. Brown, W. D. M. Rae, *Nuclear Data Sheets* 120 (2014) 115.
- [17] B. A. Brown, N. J. Stone, J. R. Stone, I. S. Towner, and M. Hjorth-Jensen, *Phys. Rev. C* 71, 044317 (2005).
- [18] P. Pirinen, J. Suhonen, and E. Ydrefors, *Physical Review C*, 99 (1), 014320 (2019).
- [19] J. Toivanen and J. Suhonen, *J. Phys. G.* 21, 1491 (1995).
- [20] J. Toivanen and J. Suhonen, *Phys. Rev. C* 57, 1237. (1998).
- [21] N. B. Gove and M. J. Martin, *Atom. Data Nucl. Data Tables* 10, 205 (1971).
- [22] J. T. Suhonen, *Frontiers in Physics* 5, 55 (2017).
- [23] J. N. Bahcall A. M. Serenelli, and S. Basu, *Astrophys. J.* 621, L85 (2005).
- [24] M. Agostini et al. (The Borexino Collaboration), *Nature* 562, 505 (2018).
- [25] A.Sh.Georgadze, et al. *Astroparticle Physics* **953**,173(1997).
- [26] J. Aalbers et al., *Eur. Phys. J. C* **77**,881(2017).
- [27] D. S. Akerib et al. *Nucl. Inst. Meth. A:* **953**,163047(2020).
- [28] J. Aalbers et al., *JCAP* **11**,017(2016).